AgriEngineering

MDPI

Article

Drying Kinetics, Effective Moisture Diffusivity, and Thermodynamic Analysis of Banana Slices Under Potassium Metabisulfite (KMS) Pretreatment

Kushal P. Dhake [1,2], Sanjay Kumar Jain [3], Pankaj B. Pathare [4,*] and Sandip D. Patil [5]

[1] Section of Agricultural Engineering, Government College of Agriculture, Mahatma Phule Krishi Vidyapeeth, Rahuri 413722, India; kpdhake@gmail.com
[2] Department of Agricultural Engineering, SVKM's College of Agriculture (Affiliated to Mahatma Phule Krishi Vidyapeeth), Shirpur 425421, India
[3] Department of Processing and Food Engineering, College of Technology and Engineering, Maharana Pratap University of Agriculture and Technology, Udaipur 313001, India
[4] Department of Soils, Water and Agricultural Engineering, College of Agricultural & Marine Sciences, Sultan Qaboos University, Muscat 123, Oman
[5] Section of Agricultural Extension, Government College of Agriculture, Mahatma Phule Krishi Vidyapeeth, Rahuri 413722, India
* Correspondence: pankaj@squ.edu.om

Abstract

The present study investigates the effect of drying temperature and potassium metabisulfite (KMS) pretreatment on the drying kinetics, effective moisture diffusivity, activation energy, thermodynamic properties, and thin-layer drying-model performance of green banana slices. Banana slices (4 ± 0.5 mm thickness) were subjected to KMS pretreatments at concentrations of 0 (control), 0.5%, 1.0%, and 1.5%, followed by drying in a convective tray dryer at 40, 50, 60, and 70 °C. The drying process exhibited a predominantly falling-rate period. Effective moisture diffusivity ranged from 2.04×10^{-10} to 4.35×10^{-10} m^2/s and increased with drying temperature. Apparent activation energy decreased from 16.19 kJ/mol for the untreated control to 13.46 kJ/mol at 1.5% KMS. Thermodynamic analysis gave enthalpy values of 10.61–13.59 kJ/mol, entropy values of −209.15 to −219.72 J/mol·K, and Gibbs free energy values of 76.35–87.73 kJ/mol. The positive ΔG values indicate that moisture removal was non-spontaneous under the investigated conditions and required external thermal-energy input. Ten thin-layer models were evaluated using R^2, RMSE, and χ^2; the Midilli–Kucuk model gave the best overall fit within the investigated temperature and KMS ranges. Because endpoint moisture contents differed among treatments, drying-time comparisons were additionally standardised to an interpolated moisture content of 10% d.b.

Keywords: green banana; pretreatment; hot air drying; moisture diffusivity; activation energy; modelling; thermodynamic analysis

Check for updates

Academic Editor: Khaled Abdel Salam El-Sayed Metwally

Received: 1 July 2026
Revised: 30 August 2026
Accepted: 1 September 2026
Published: 7 September 2026

Copyright: © 2026 by the authors. Licensee MDPI, Basel, Switzerland. This article is an open access article distributed under the terms and conditions of the Creative Commons Attribution (CC BY) license.

1. Introduction

Banana (*Musa* spp.) is an important tropical fruit crop, while green bananas are particularly susceptible to postharvest deterioration because of their high moisture content and physiological activity [1,2]. Processing green bananas into dried slices and flour can extend product usability and create value-added food ingredients. Banana flour has been investigated for bakery and other food applications because of its starch, dietary fibre and

functional characteristics [3–5]. Drying performance is governed by interacting factors, including air temperature, air velocity, sample geometry, tissue structure, initial moisture content and pretreatment. These factors influence both the external heat-transfer driving force and the internal resistance to moisture migration; consequently, their combined effect should be considered when interpreting drying kinetics [6].

Unripe banana flour can also be incorporated into value-added products such as slowly digestible cookies and high-fibre breads [7]. Such applications increase the potential utilisation of fruit that may otherwise have limited market value at the green stage.

Drying is an established preservation method for bananas because it reduces moisture availability and facilitates handling, storage and transportation [8]. However, drying can also be energy-intensive and may cause undesirable changes in colour, texture and nutritional quality if conditions are not appropriately selected [3]. Mathematical descriptions of convective drying based on diffusion theory are widely used to represent moisture-transfer behaviour and to estimate effective moisture diffusivity [9,10]. Drying-kinetics analysis provides parameters that can support drying-time estimation and equipment/process design [10]. Mathematical models are therefore useful for comparing drying behaviour and selecting an empirical representation of moisture-ratio data [9]. Pretreatment can further modify drying by altering tissue permeability and reducing resistance to moisture migration, while also helping to control browning and other quality changes [11,12].

Recent reviews demonstrate that banana drying research encompasses a wide range of pretreatments and drying technologies, but comparatively fewer studies have integrated pretreatment concentration with effective moisture diffusivity, activation energy, thermodynamic parameters and systematic comparison of multiple thin-layer models under the same controlled convective-drying conditions [13]. The present study therefore focuses on the mechanistic interpretation of drying rather than repeating a process-optimisation exercise. The novelty lies in linking KMS concentration (0–1.5%) and drying temperature (40–70 °C) with (i) drying-rate behaviour, (ii) apparent effective moisture diffusivity obtained from the approximately linear long-time ln(MR) region, (iii) activation energy, (iv) thermodynamic parameters, and (v) comparative evaluation of ten thin-layer models. This integrated approach provides a transport- and energy-based interpretation of KMS-assisted drying of green banana slices and establishes a common-moisture basis for comparing drying times.

2. Materials and Methods

2.1. Materials

Green banana cv. *Nendran* at stage 2 maturity were procured from the local Savina market of Udaipur, Rajasthan, India. The bananas were washed under tap water to remove dust, dirt and unwanted material. The cleaned bananas were peeled using a sharp-edged knife and the peel was removed completely. The peeled bananas were sliced using a hand slicer to a thickness of 4 ± 0.5 mm. Approximately 100 g of peeled green banana slices were used for each treatment, and three independent replicates were conducted for each treatment. Moisture content was determined by drying samples in a hot-air oven at 105 °C until constant mass; three analytical determinations were performed for each moisture-content measurement [14]. Initial moisture content was recorded before drying, and final moisture content was determined at the end of each drying run using the same oven-drying procedure. The initial moisture content varied among the experimental batches; therefore, the manuscript reports the experimental range rather than assigning a single value to all treatments.

2.2. Pre-Treatment

Pretreatments are commonly used to reduce browning and modify the drying behaviour of fruits and vegetables [11,12]. In green banana processing, pretreatment can influence the colour and physicochemical properties of the resulting flour [15]. KMS and citric acid are among the chemical pretreatments reported for banana and other fruit products [12,16].

In the present study, green banana slices were treated with 0.5%, 1.0% and 1.5% potassium metabisulfite (KMS) for 10 min before drying, while untreated slices served as the control. The 10 min treatment duration was selected in accordance with previously reported banana pretreatment protocols [12,16].

2.3. Tray Drying

Convective drying experiments were conducted in a laboratory tray dryer (Figure 1) (Model 12 TD, Lab Line, Vadodara, Gujarat, India) equipped with four electrical heaters and forced-air circulation. The chamber temperature was controlled to within ±1 °C, and air velocity was maintained at 2.5 m/s. The experimental procedure used for the preparation and drying of green banana slices is presented as a process flow diagram in Figure 2. Drying temperatures of 40, 50, 60 and 70 °C were investigated. Before loading the samples, the dryer was operated for 30 min to establish the target temperature. Peeled banana slices were uniformly distributed on stainless-steel trays to avoid overlap. The sample mass was recorded at regular intervals using a digital weighing balance with an accuracy of 0.01 g. The drying curves represent the mean moisture-content response of the replicate experimental observations.

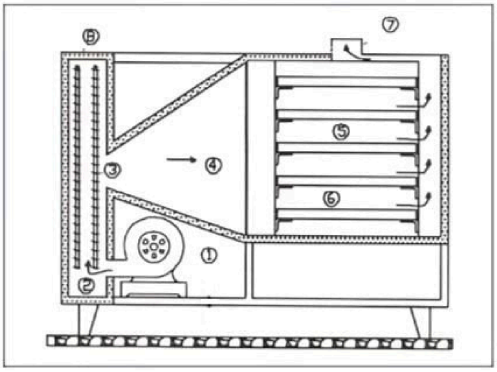


Figure 1. Internal details of the laboratory tray dryer used for drying green banana slices. Arrow stands for air circulation direction.

Three replicate experimental observations were used for the moisture-content measurements, with three analytical determinations for each moisture-content value. The derived drying-model and transport parameters were calculated from the mean moisture-ratio trajectory. Because replicate-level raw drying curves were not available in the revised manuscript file, standard deviations for the derived parameters are not reported; this is identified as a limitation rather than estimated from the mean curve.

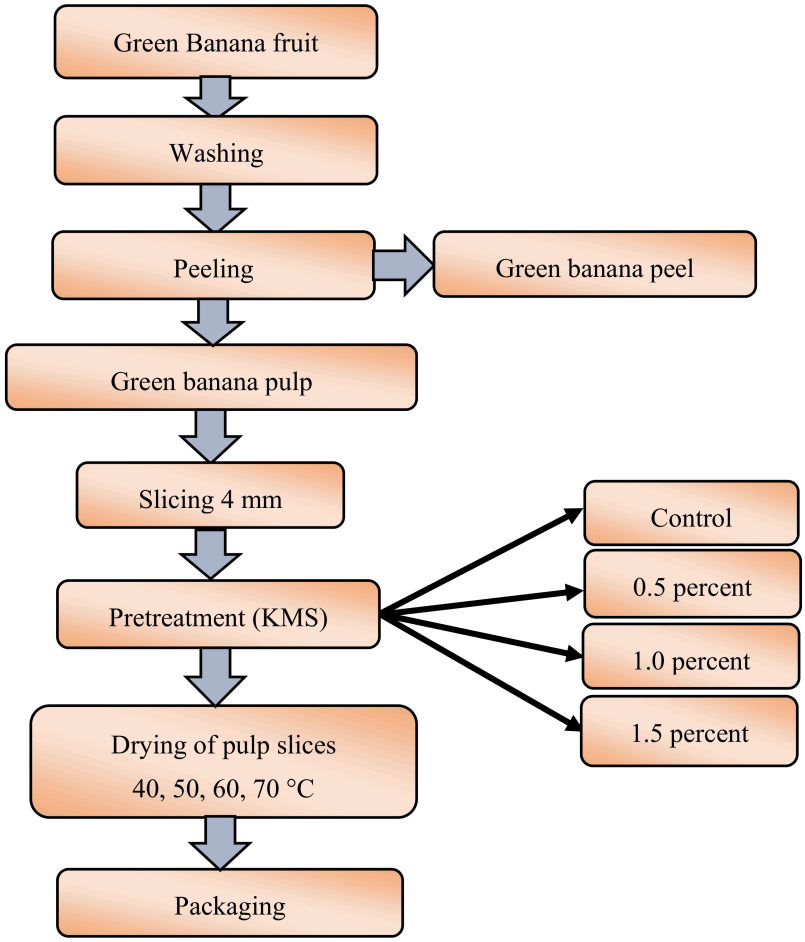


Figure 2. Process flow diagram of banana slice drying.

2.4. Drying Characteristics

2.4.1. Moisture Ratio

The moisture ratio (MR) was calculated from the moisture content at a given time relative to the initial and equilibrium moisture contents using Equation (1), as recommended for thin-layer drying analysis [4,16]. The equilibrium moisture content (Me) was not directly measured in the tray-drying experiments. Therefore, for the present calculations, Me was assumed to be negligible relative to M and M_0, giving the simplified relationship $MR \approx M/M_0$. This assumption is explicitly stated because Me was not experimentally determined and the experiments were continued well below the initial moisture level.

$$MR = \frac{(M - M_e)}{(M_0 - M_e)} \quad (1)$$

where

M—Moisture content at time, (% d.b.);
M_0—Initial moisture content, (% d.b.);
Me—Equilibrium moisture content, (% d.b.).

2.4.2. Drying Rate

The moisture-content data were used to determine moisture loss during each elementary drying interval. The drying rate of green banana slices was calculated from the mass balance in Equation (2):

$$R = \frac{\Delta m_w}{(\Delta t \cdot m_d)} \quad (2)$$

where

R—Drying rate, g water/(g dry matter·min);
Δm_v—Mass of water evaporated during the interval, g;
Δt—Elapsed drying-time interval, min;
m_d—Mass of bone-dry solid matter, g.

2.4.3. Moisture Diffusivity

The green banana slices were treated as an infinite slab with a nominal thickness of 4 mm for application of the Fickian diffusion solution for an infinite slab [17].

$$MR = \frac{8}{\pi^2} \sum_{n=0}^{\infty} \frac{1}{(2n+1)^2} \exp\left[\frac{-(2n+1)^2 \pi^2 D_{eff}.t}{L^2}\right] \quad (3)$$

where

MR—Moisture ratio, dimensionless;
D_{eff}—Effective diffusivity, m^2/s;
L—Characteristic dimension, i.e., thickness of slab, m;
t—Time elapsed during drying, s.

Effective moisture diffusivity (D_{eff}) was obtained from the slope of the approximately linear long-time portion of the ln(MR) versus drying-time relationship. The complete ln(MR) curves were not assumed to be linear. For each temperature–pretreatment combination, only the approximately linear long-time region was fitted by linear regression; the fitted slope was then converted to Deff using the infinite-slab relationship. Thus, the reported values are apparent effective diffusivities and should not be interpreted as constant molecular diffusivities throughout the entire drying trajectory.

$$\text{Slope} = \frac{\pi^2 D_{eff}.t}{L^2} \quad (4)$$

2.4.4. Thermodynamic Properties

Thermodynamic parameters were estimated from the Arrhenius activation energy obtained from the slope of $\ln(D_{eff})$ versus $1/T$. Enthalpy was calculated as $\Delta H = E_a - RT$, entropy was obtained from the Eyring relationship, and Gibbs free energy was calculated as $\Delta G = \Delta H - T\Delta S$ [18]. These are apparent thermodynamic quantities derived from the drying model and describe the temperature dependence of moisture transport.

$$\Delta H = E_a - RT \quad (5)$$

$$\Delta S = R\left(\ln D_0 - \ln \frac{k_b}{h_p} - \ln T\right) \quad (6)$$

$$\Delta G = \Delta H - T\Delta S \quad (7)$$

where

ΔH—Variation in enthalpy (J/mol);
ΔG—Variation in Gibbs free energy (J/mol);
R—Universal gas constant (8.314 J/mol K);
h_p—Planck constant (6.626×10^{-34} Js);
ΔS—Variation in entropy (J/mol K);
k_b—Boltzmann constant (1.38×10^{-23} J/K);
T—Absolute temperature (K);
E_a—Activation energy (J/mol);

D_0—Pre-exponential factor (m^2/s).

2.4.5. Mathematical Modelling

Ten commonly used thin-layer drying models—Page, Henderson–Pabis, Logarithmic, Newton, Two-term, Two-term exponential, Wang and Singh, Diffusion approximation, Verma et al., and Midilli–Kucuk—were fitted to the experimental moisture-ratio data (Table 1). Model parameters were estimated by nonlinear regression in Microsoft Excel. The objective was to minimise the sum of squared differences between experimental and predicted MR values. Model adequacy was assessed jointly using R^2, reduced chi-square (χ^2), and RMSE; higher R^2 and lower χ^2 and RMSE indicated closer agreement. Because the models were fitted and assessed using the same dataset, these statistics are treated as goodness-of-fit indicators rather than independent validation statistics.

Table 1. Mathematical models used by different authors in drying of food materials.

Sr. No		Mathematical Equation	Reference
1	Page	$MR = e^{(-kt^n)}$	[19]
2	Henderson and Pabis	$MR = a\, e^{(-kt)}$	[20]
3	Logarithmic	$MR = a\, e^{(-kt)} + C$	[19]
4	Newton	$MR = exp(-kt)$	[6]
5	Two–term	$MR = a\, exp(-k_0 t) + b\, exp(-k_1 t)$	[19]
6	Two–term exponential	$MR = a\, exp(-kt) + (1 - a) exp(-kat)$	[21]
7	Wang & Singh	$MR = 1 + at + bt^2$	[19]
8	Diffusion approach	$MR = a\, exp(-kt) + (1 - a) exp(-kbt)$	[19]
9	Verma	$MR = a\, exp(-kt) + (1 - a) exp(-gt)$	[21]
10	Midilli–Kucuk	$MR = a\, exp(-kt^n) + bt$	[19]

where k—drying rate constant; n—dimensionless empirical coefficient; t—drying time, min; a and C—empirical constants in drying models.

The models were fitted and evaluated using the same experimental dataset. R^2, χ^2 and RMSE were used as descriptive measures of goodness of fit rather than as independent validation statistics. The three criteria were considered jointly, with higher R^2 and lower χ^2 and RMSE indicating closer agreement between measured and model-predicted moisture ratios.

$$\chi^2 = \frac{\sum_{i=1}^{N} \left(M_{R,exp,i} - M_{R,pre,i}\right)^2}{N - z} \quad (8)$$

$$RMSE = \left[\frac{1}{N}\sum_{i=1}^{N} \left(M_{R,exp,i} - M_{R,pre,i}\right)^2\right]^{1/2} \quad (9)$$

where M_R,exp,i and M_R,pre,i are the experimental and predicted dimensionless moisture ratios, respectively, and N is the number of observations; and z is the number of drying constants.

3. Results and Discussion

3.1. Effect on Drying Characteristics of Green Banana Slices

Moisture content decreased rapidly during the early stage of drying and subsequently declined more gradually, producing a predominantly falling-rate profile across the investigated conditions (Figure 3). The observed endpoint drying times ranged from 270 to 480 min, while final moisture contents differed among treatments (5.95–8.95% d.b.). Consequently, endpoint drying time was not used alone to rank treatment effectiveness. The drying-time observations were previously reported in a process-optimisation study [16]; in the present manuscript, they are retained only as the experimental basis for the subsequent drying-rate, diffusivity, activation-energy, thermodynamic and modelling analyses.

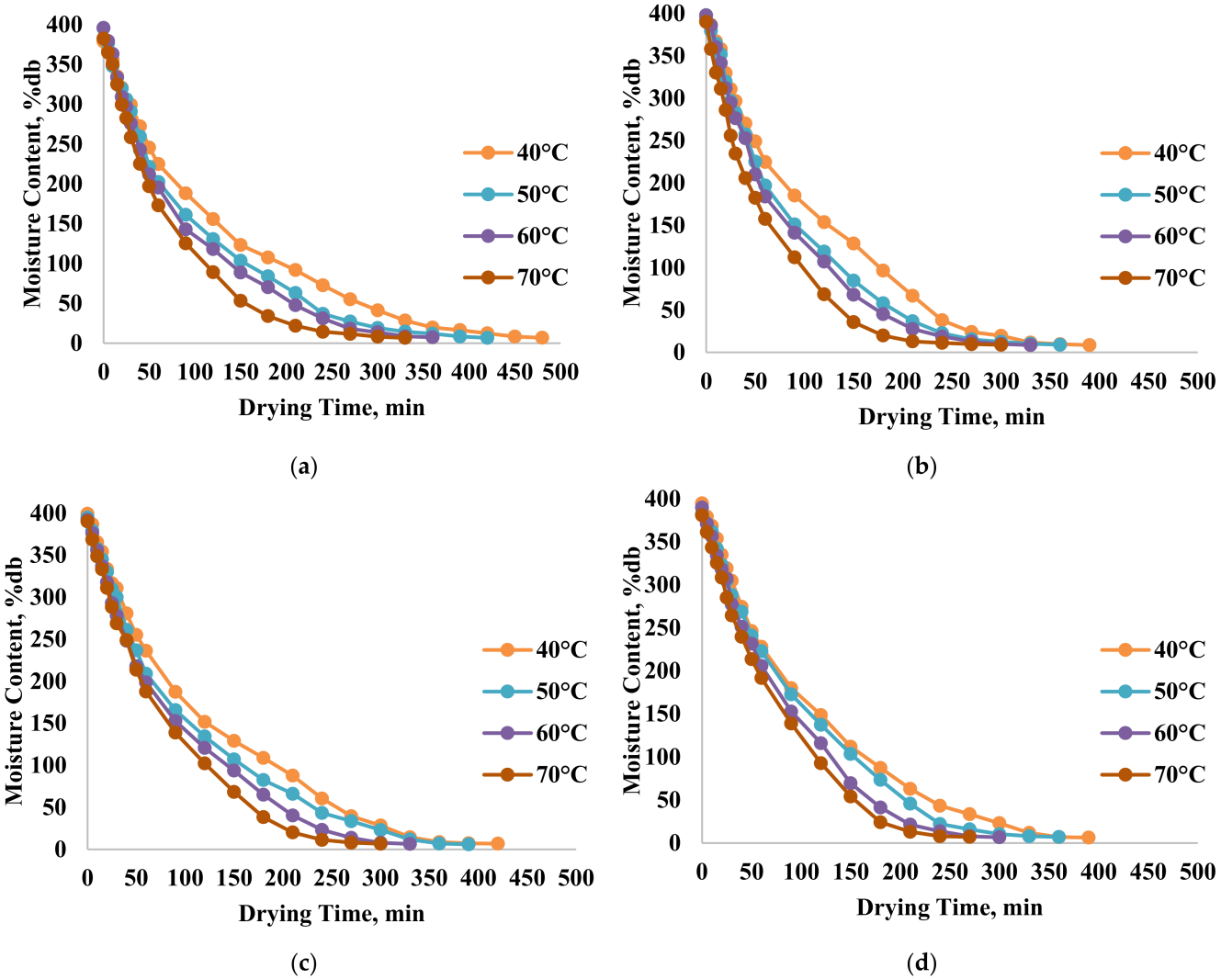


Figure 3. Variation in the moisture content with drying time for (**a**) untreated (control) and KMS-treated green banana slices, i.e., (**b**) 0.5% KMS, (**c**) 1.0% KMS, and (**d**) 1.5% KMS, at various drying air temperatures.

The reduction in drying time with increasing air temperature is consistent with the greater external heat-transfer driving force and enhanced moisture mobility at higher temperatures [6,22–24]. However, because the endpoint moisture contents were not identical, differences in total endpoint time should not be interpreted as direct evidence of a proportional improvement in drying efficiency. A common-moisture comparison is therefore provided below.

Figure 3 shows an inverse relationship between drying time and drying air temperature; i.e., as the drying air temperature rises, the drying time decreases. This indicates that as the drying air temperature increased, the rate of moisture removal also increased. Drying is a simultaneous heat- and mass-transfer process in which higher drying air temperatures enhance heat transfer and accelerate moisture migration.

At 40 and 50 °C, green banana slices generally required longer periods to approach their experimental endpoints than at 60 and 70 °C. This behaviour is consistent with reported convective drying studies of banana slices, where increasing air temperature accelerates moisture removal and shortens the time required to reach a specified moisture level [6,22–24]. The present results are therefore interpreted primarily in terms of the drying trajectory and moisture-transfer mechanism rather than the endpoint time alone.

3.2. Effect of Pre-Treatment on Drying of Green Banana Slices

KMS pretreatment altered the drying response relative to the untreated control (Figure 4). The 0.5% KMS treatment generally produced the shortest drying trajectory among the pretreatments, whereas increasing the concentration to 1.0 and 1.5% did not produce a proportional further reduction. Similar concentration-dependent pretreatment effects have been reported for banana and other fruit materials [12,16,25]. Chemical pretreatment can modify tissue permeability and the resistance to internal moisture movement, but the response need not increase linearly with concentration [11,26].

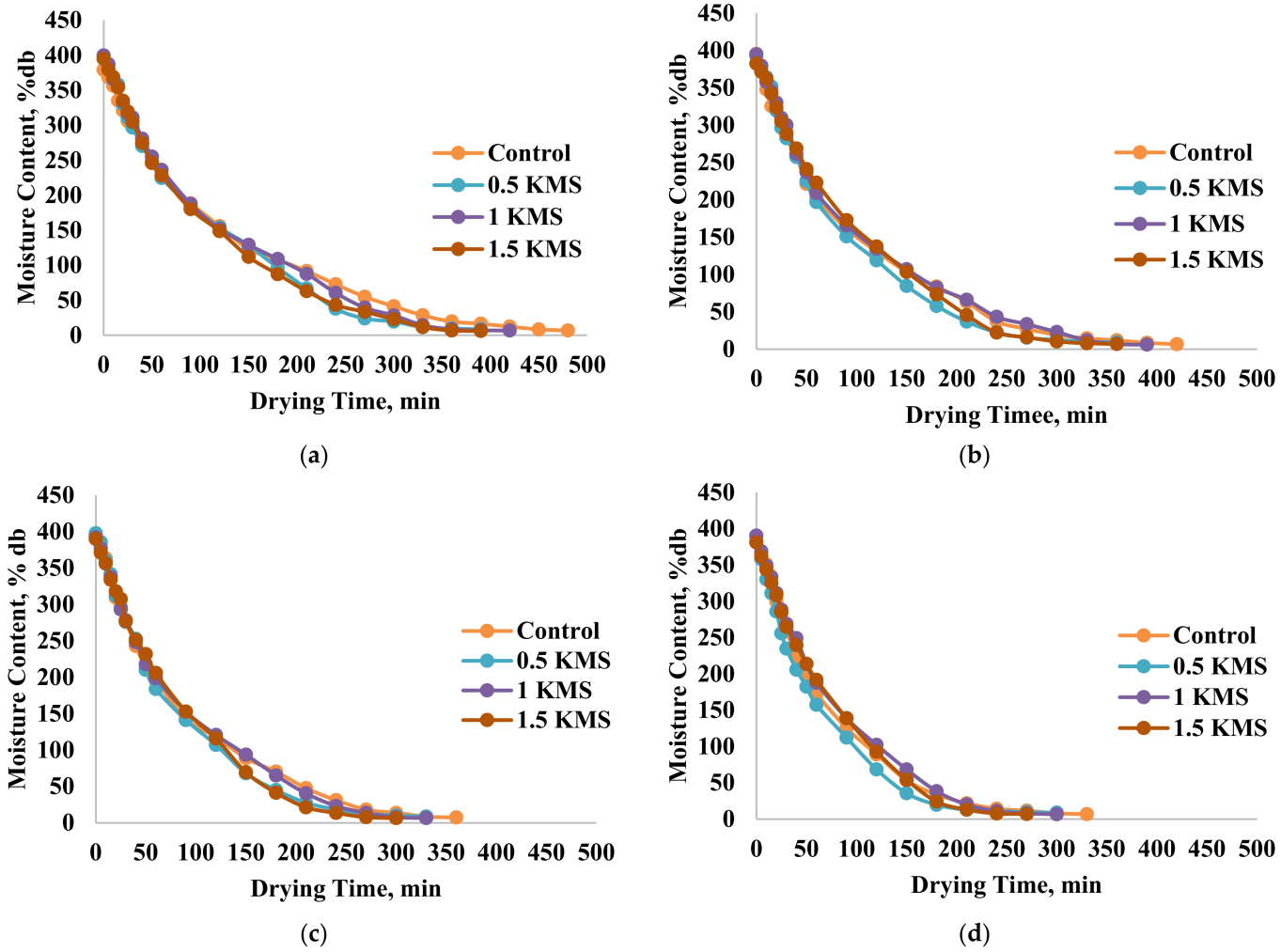


Figure 4. Variation in the moisture content with drying time for various pretreatments of green banana slices at (**a**) 40, (**b**) 50, (**c**) 60, and (**d**) 70 °C drying air temperatures.

At lower air temperatures, the time required to reach the experimental endpoint was longer, whereas higher temperatures accelerated moisture removal. Figure 4 compares the four KMS levels at each drying temperature and shows that the pretreatment effect was condition-dependent rather than a simple monotonic function of concentration.

At 40 °C, untreated banana slices required 480 min to reach 6.80% d.b. from an initial moisture content of 378.86% d.b. At the same temperature, the 0.5%, 1.0% and 1.5% KMS treatments required 390, 420 and 390 min, respectively, to reach their experimental endpoints. These endpoint times are reported only to illustrate the observed treatment response because final moisture contents differed among treatments. Similar temperature-dependent trends were observed at 50, 60 and 70 °C.

The effect of drying temperature is consistent with previous banana-drying studies. For example, Kumar et al. reported that increasing drying temperature enhanced the drying rate of banana slices, while Macedo et al. similarly observed accelerated moisture removal at higher air temperatures [6,23,24]. The present study extends these observations by quantifying the associated change in apparent moisture diffusivity and activation energy under different KMS concentrations.

KMS pretreatment reduced the observed endpoint drying time relative to the untreated control, which may be associated with altered tissue permeability and reduced resistance to internal moisture migration [11,12,16]. However, the endpoint moisture contents differed among treatments; therefore, endpoint time alone is not sufficient to quantify the magnitude of the pretreatment effect.

Figure 4 compares the moisture-content trajectories for the four KMS levels at each drying temperature. The curves show that KMS pretreatment modified the drying response, but the differences among concentrations were not uniformly proportional throughout the drying process. Accordingly, the discussion focuses on the observed kinetic differences and their implications for moisture transport rather than repeating the complete experimental dataset.

To provide a common basis for comparison despite the different experimental endpoints, drying time was also evaluated at an interpolated moisture content of 10% d.b. Across the investigated temperature–KMS combinations, the interpolated time to 10% d.b. ranged from 227.0 to 437.6 min. This common-moisture comparison provides a more consistent basis for comparing treatment conditions than endpoint drying time alone. The economic significance of the observed time reduction cannot be quantified from the present dataset because electrical energy consumption, specific energy consumption and operating cost were not measured.

3.3. Effect of Air Temperature and Pre-Treatment on Drying Rate of Green Banana Slices

The drying behaviour was further analysed using drying-rate curves (Figure 5), which demonstrate the absence of a measurable constant-rate period and indicate that drying occurred predominantly in the falling-rate period.

Increasing air temperature increased the drying rate and shortened the time required for dehydration. KMS pretreatment also modified the drying-rate profile. The highest initial drying rate at 70 °C was observed for the 0.5% KMS treatment. This agrees with the previously reported maximum initial drying rate of approximately 0.046 g water/(g dry matter·min) for 0.5% KMS-treated green banana slices [16]. The concentration-dependent response indicates that increasing KMS concentration does not necessarily produce a proportional increase in drying rate.

The initial drying rate was highest when readily available moisture was abundant. As drying progressed, the rate decreased because the remaining water had to migrate through an increasingly moisture-depleted internal matrix, increasing the resistance to transport [27–29]. The continuous decline in drying rate therefore supports the interpretation that internal moisture movement becomes increasingly important during the later stages of dehydration.

The absence of a measurable constant-rate period and the continuous decline in drying rate indicate that internal moisture movement provided important resistance over the investigated range. Similar falling-rate behaviour has been reported for banana and plantain materials [20,23,29,30]. In the present study, this observation provides the physical basis for estimating apparent effective moisture diffusivity.

As moisture content decreased, the corresponding drying rate also decreased. This behaviour can be attributed to the decreasing availability of free moisture and the increasing

resistance to movement of moisture from the inner regions of the slice to the surface [27–31]. The present observations are therefore consistent with diffusion-dominated drying reported for banana-based materials.

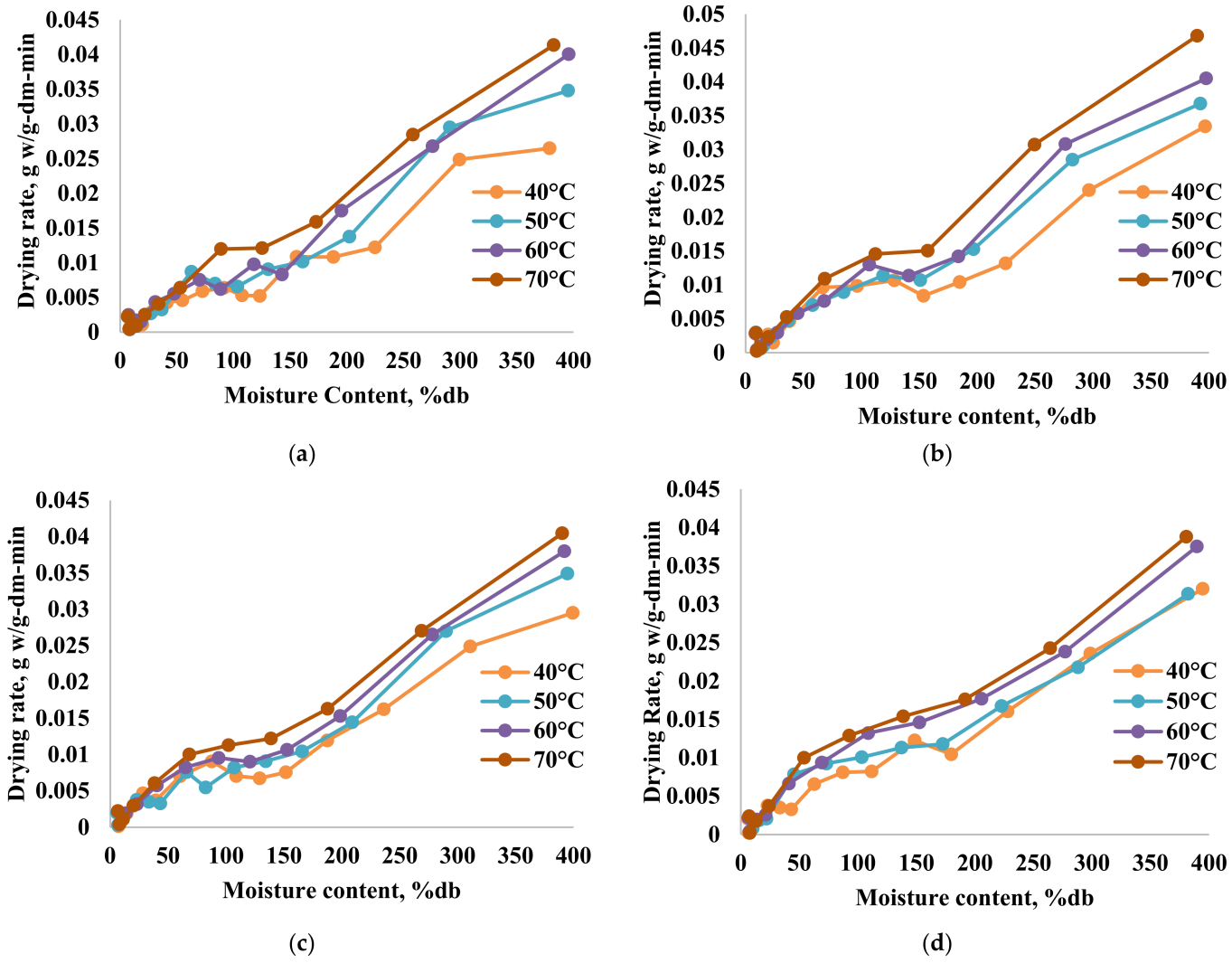


Figure 5. Relationship between drying rate and moisture content for banana slices dried, i.e., (**a**) untreated (control), (**b**) 0.5% KMS, (**c**) 1.0% KMS, and (**d**) 1.5% KMS, at various drying air temperatures.

3.4. Moisture Diffusivity (D_{eff}) of Green Banana Slices

The continuous falling-rate behaviour indicates that internal moisture transport provides important resistance during drying. Accordingly, apparent effective moisture diffusivity (Deff) was estimated from the linearised moisture-ratio relationship described in Section 2.4.3. The resulting values provide a comparative measure of apparent internal moisture-transfer capacity under each temperature and pretreatment condition.

Figure 6 presents ln(MR) as a function of drying time. The complete curves were not perfectly linear over the entire drying period, reflecting changes in moisture-transfer resistance during dehydration. Therefore, Deff was calculated only from the approximately linear long-time region. The curvature outside this region may reflect changing moisture binding, tissue shrinkage and pretreatment-dependent transport resistance. This distinction resolves the apparent contradiction between a nonlinear overall drying trajectory and the use of a local linear slope for the Fickian approximation.

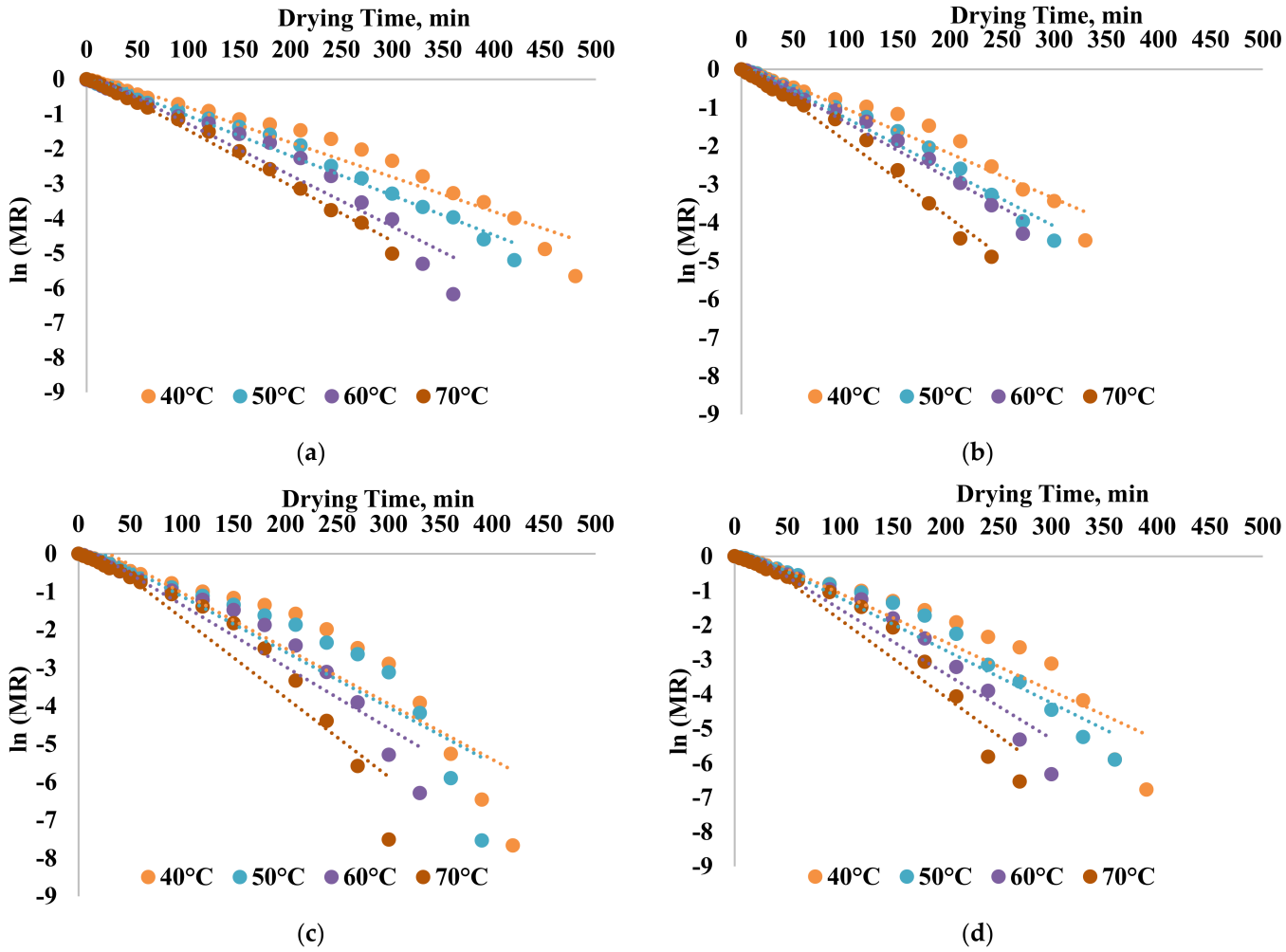


Figure 6. Variation in ln (MR) with time for green banana slices for different temperatures for (**a**) untreated (control) and KMS-treated green banana slices, i.e., (**b**) 0.5% KMS, (**c**) 1.0% KMS, and (**d**) 1.5% KMS.

The modified slope method was used to calculate apparent effective moisture diffusivity (Deff) during convective drying of control and KMS-treated banana slices. The values for the different drying-air temperatures and pretreatment combinations are presented in Table 2. Deff increased with temperature, indicating enhanced apparent moisture mobility and reduced internal resistance. The present values (2.04×10^{-10}–4.35×10^{-10} m^2/s) are comparable with the 2.04×10^{-10}–4.35×10^{-10} m^2/s range reported previously for the same green-banana/KMS system [16], while studies on other banana cultivars and drying configurations have reported different diffusivity levels because of differences in cultivar, thickness, pretreatment and drying conditions [23,32]. Thus, direct numerical comparison should be made only when geometry and drying conditions are comparable.

Across the investigated conditions, apparent effective moisture diffusivity ranged from 2.04×10^{-10} to 4.35×10^{-10} m^2/s. These values fall within the broad range commonly reported for food materials. The temperature-dependent increase is consistent with greater molecular mobility at higher temperatures, while differences among KMS treatments may reflect changes in tissue permeability and internal moisture-transfer resistance [11,16,32,33].

The analysis of variance (ANOVA) for diffusivity is presented in Table 3. Both drying temperature and KMS pretreatment had significant effects on apparent moisture diffusivity at the 1% significance level. The ANOVA supports the observed treatment trends, although

the derived diffusivity values should be interpreted as apparent parameters because they depend on the selected linearisation region and the infinite-slab approximation.

Table 2. Effective moisture diffusivity in tray drying of green banana slices.

Sr. No.	Pre-Treatment, %, KMS	Temperature, °C	Effective Diffusivity, m^2/s
1	Control	40	2.04×10^{-10}
2	Control	50	2.51×10^{-10}
3	Control	60	2.70×10^{-10}
4	Control	70	3.65×10^{-10}
5	0.5 KMS	40	2.54×10^{-10}
6	0.5 KMS	50	3.07×10^{-10}
7	0.5 KMS	60	3.32×10^{-10}
8	0.5 KMS	70	4.35×10^{-10}
9	1.0 KMS	40	2.21×10^{-10}
10	1.0 KMS	50	2.45×10^{-10}
11	1.0 KMS	60	2.93×10^{-10}
12	1.0 KMS	70	3.57×10^{-10}
13	1.5 KMS	40	2.48×10^{-10}
14	1.5 KMS	50	2.88×10^{-10}
15	1.5 KMS	60	3.50×10^{-10}
16	1.5 KMS	70	3.84×10^{-10}

Table 3. ANOVA for the effects of drying-air temperature and KMS pretreatment on effective moisture diffusivity.

S.V.	SS	df	MS	F	*p*-Value	F-Value	Test
Pretreatment	1.271×10^{-16}	3	4.24×10^{-17}	17.13	0.000461	6.99	*
Temperature	3.214×10^{-16}	3	1.07×10^{-16}	43.30	1.13×10^{-5}	6.99	*
Error	2.226×10^{-17}	9	2.47×10^{-18}				
Total	4.708×10^{-16}	15					

*—significant at a 1% level.

3.5. Activation Energy

The activation energy for thin-layer drying of green banana slices was calculated using an Arrhenius-type equation based on the slope of ln(Deff) versus the reciprocal of absolute temperature (1/T). The activation-energy values for the different pretreatments are presented in Table 4.

Table 4. Activation energy for tray drying of green banana slices.

Sr. No.	Pretreatment, %, KMS	Activation Energy
1	Control	16.19 kJ/mol
2	0.5 KMS	15.06 kJ/mol
3	1.0 KMS	14.43 kJ/mol
4	1.5 KMS	13.46 kJ/mol

The untreated samples showed the highest activation energy (16.19 kJ/mol). Increasing KMS concentration reduced Ea to 15.06, 14.43 and 13.46 kJ/mol for 0.5, 1.0 and 1.5% KMS, respectively. The progressive reduction indicates a lower apparent energetic barrier for

moisture transport after pretreatment. Similar reductions in apparent activation energy following pretreatment have been reported for food materials where pretreatment modifies moisture-transfer resistance [11,27].

The inverse relationship between KMS concentration and Ea indicates that the apparent temperature sensitivity of moisture transport decreased after pretreatment. The Ea values obtained here are within the range reported for biological materials, including convectively dried plantain [27]. The result provides a mechanistic complement to the previous optimisation study [16] by linking KMS concentration with the apparent energy requirement of moisture transport.

3.6. Thermodynamic Properties of Dried Banana Slices

Thermodynamic parameters provide an additional description of the energetic characteristics of moisture transport. ΔH decreased slightly with increasing temperature because $\Delta H = E_a - RT$; this indicates that the enthalpic requirement associated with the activated transport process becomes slightly smaller at a higher temperature (Table 5). The negative ΔS values indicate a decrease in entropy between the initial and activated states, consistent with a more ordered activated configuration for moisture transport. The positive ΔG values indicate that moisture removal was non-spontaneous under the investigated conditions and therefore required external thermal energy input. Importantly, these are apparent thermodynamic parameters derived from the drying model and should not be interpreted as direct measurements of molecular-scale structural changes.

Table 5. Thermodynamic properties of green banana slices during drying.

Treatment	Temp (°C)	Temp (K)	ΔH (kJ/mol)	ΔS (J/mol·K)	ΔG (kJ/mol)
Control	40	313.15	13.59	−215.63	81.11
	50	323.15	13.50	−216.02	83.31
	60	333.15	13.42	−216.41	85.52
	70	343.15	13.34	−216.79	87.73
0.5% KMS	40	313.15	12.46	−218.45	80.86
	50	323.15	12.37	−218.87	83.10
	60	333.15	12.29	−219.30	85.35
	70	343.15	12.21	−219.72	87.60
1% KMS	40	313.15	11.83	−212.84	78.48
	50	323.15	11.74	−213.25	80.66
	60	333.15	11.66	−213.66	82.84
	70	343.15	11.58	−214.07	85.04
1.5% KMS	40	313.15	10.86	−209.15	76.35
	50	323.15	10.77	−209.56	78.49
	60	333.15	10.69	−209.97	80.64
	70	343.15	10.61	−210.38	82.80

The enthalpy values ranged from 10.61 to 13.59 kJ/mol across the investigated treatments and temperatures. For the control, ΔH decreased from 13.59 to 13.34 kJ/mol as temperature increased from 40 to 70 °C; for 0.5% KMS, the values were 12.46–12.21 kJ/mol; for 1.0% KMS, 11.83–11.58 kJ/mol; and for 1.5% KMS, 10.86–10.61 kJ/mol. The positive ΔG values indicate non-spontaneous moisture removal, while the negative ΔS values indicate

a decrease in entropy of the activated state. These quantities should be interpreted as apparent model-derived parameters.

3.7. Modelling of Drying Curves

The experimental moisture-ratio data were fitted to ten thin-layer drying equations to determine which empirical representation most closely described the observed drying behaviour. The models were fitted using the same experimental observations, and their performance was compared using R^2, RMSE and χ^2.

The drying constants and statistical parameters, including R^2, RMSE and reduced χ^2, for the evaluated mathematical models are presented in Table 6. Overall R^2 values ranged from 0.9567 to 0.9991, while RMSE and χ^2 ranged from 0.0112 to 0.07219 and 0.00016 to 0.00573, respectively. The Midilli–Kucuk model provided the best overall representation according to the combined criteria (Figure 7), but this conclusion is limited to the investigated temperature and KMS ranges and should not be interpreted as universal superiority under all drying conditions. Its good performance is consistent with previous banana-drying studies in which flexible semi-empirical models adequately represented the falling-rate behaviour [13,20,23,34]. Because all models were fitted and assessed using the same experimental dataset, the reported statistics describe goodness of fit rather than independent predictive validation.

Table 6. Thin-layer drying model constants and goodness-of-fit statistics for green banana slices.

Model	Pretreatment, % KMS	Air Temp., °C	Parameters	R^2	RMSE	χ^2
Newton	0	40	k = 0.00786	0.9970	0.01949	0.000397
	0	50	k = 0.01021	0.9958	0.02253	0.000532
	0	60	k = 0.0118	0.9946	0.02472	0.000645
	0	70	k = 0.01441	0.9922	0.03273	0.001134
	0.5	40	k = 0.00904	0.9934	0.02897	0.000881
	0.5	50	k = 0.00995	0.9853	0.04702	0.002328
	0.5	60	k = 0.01179	0.9960	0.02153	0.00058
	0.5	70	k = 0.01441	0.9922	0.03273	0.001134
	1.0	40	k = 0.00853	0.9956	0.02340	0.000574
	1.0	50	k = 0.00973	0.9974	0.01803	0.000342
	1.0	60	k = 0.01179	0.9946	0.02472	0.000645
	1.0	70	k = 0.00530	0.9928	0.03061	0.00102
	1.5	40	k = 0.00908	0.9973	0.01854	0.000361
	1.5	50	k = 0.00984	0.9965	0.0201	0.00041
	1.5	60	k = 0.01162	0.9952	0.0243	0.00058
	1.5	70	k = 0.01246	0.9933	0.02892	0.000889
Page	0	40	k = 0.00917, *n* = 0.96831	0.9972	0.01853	0.000375
	0	50	k = 0.01374, *n* = 0.93446	0.9971	0.01870	0.000384
	0	60	k = 0.0154, *n* = 0.9379	0.9959	0.02154	0.000518
	0	70	k = 0.00872, *n* = 1.1240	0.9952	0.02561	0.000738
	0.5	40	k = 0.00850, *n* = 1.01315	0.9934	0.02886	0.000921
	0.5	50	k = 0.00426, *n* = 1.19005	0.9923	0.03400	0.001284
	0.5	60	k = 0.01544, *n* = 0.93789	0.9976	0.01672	0.00037
	0.5	70	k = 0.00872, *n* = 1.12401	0.9952	0.02561	0.000738
	1.0	40	k = 0.00872, *n* = 0.99527	0.9956	0.02339	0.000602
	1.0	50	k = 0.01038, *n* = 0.98600	0.9974	0.01784	0.000352
	1.0	60	k = 0.01544, *n* = 0.93789	0.9959	0.02154	0.000518

Table 6. *Cont.*

Model	Pretreatment, % KMS	Air Temp., °C	Parameters	R^2	RMSE	χ^2
	1.0	70	k = 0.00000, *n* = 30.12982	0.9965	0.02059	0.00047
	1.5	40	k = 0.00749, *n* = 1.04134	0.9978	0.01687	0.000315
	1.5	50	k = 0.00872, *n* = 1.0215	0.9978	0.0179	0.00030
	1.5	60	k = 0.01488, *n* = 0.9342	0.9969	0.0210	0.00046
	1.5	70	k = 0.00755, *n* = 1.11798	0.9968	0.02003	0.000455
Henderson-Pabis	0	40	a = 0.99158, k = 0.00777	0.9971	0.01912	0.000399
	0	50	a = 0.97712, k = 0.00984	0.9966	0.02026	0.000452
	0	60	a = 0.9662, k = 0.0112	0.9965	0.01971	0.000434
	0	70	a ≈ 1.0696, k = 0.01599	0.9981	0.01600	0.000288
	0.5	40	a = 1.00203, k = 0.00907	0.9934	0.02896	0.000927
	0.5	50	a = 1.09746, k = 0.01146	0.9977	0.01851	0.000381
	0.5	60	a = 0.96624, k = 0.01116	0.9966	0.02049	0.00046
	0.5	70	a = 1.06959, k = 0.01599	0.9981	0.01600	0.000288
	1.0	40	a = 0.99600, k = 0.00848	0.9957	0.02333	0.000599
	1.0	50	a = 0.99866, k = 0.00971	0.9974	0.01802	0.000359
	1.0	60	a = 0.96624, k = 0.01116	0.9965	0.01971	0.000434
	1.0	70	a = 1.13790, k = 0.00618	0.99782	0.01611	0.00036
	1.5	40	a = 1.01263, k = 0.00925	0.9976	0.01760	0.000343
	1.5	50	a = 1.0068, k = 0.00967	0.9974	0.0185	0.00033
	1.5	60	a = 0.9723, k = 0.01098	0.9964	0.0217	0.00049
	1.5	70	a = 1.02574, k = 0.01295	0.9944	0.02642	0.000791
Logarithmic	0	40	a = 1.00469, k = 0.00735, c = −0.01890	0.9974	0.01814	0.000376
	0	50	a = 0.98049, k = 0.00969, c = −0.00522	0.9966	0.02017	0.000471
	0	60	a = 0.9844, k = 0.01037, c = −0.02618	0.9971	0.01799	0.000384
	0	70	a = 1.0785, k = 0.01546, c = −0.01345	0.9984	0.01494	0.000268
	0.5	40	a = 1.04376, k = 0.00782, c = −0.05692	0.9954	0.02413	0.000680
	0.5	50	a = 1.10978, k = 0.01095, c = −0.01814	0.9980	0.01719	0.000348
	0.5	60	a = 0.98437, k = 0.01037, c = −0.02618	0.9979	0.01537	0.00031
	0.5	70	a = 1.07852, k = 0.01546, c = −0.01345	0.9984	0.01494	0.000268
	1.0	40	a = 1.03003, k = 0.00747, c = −0.04699	0.9971	0.01907	0.000421
	1.0	50	a = 1.00935, k = 0.00929, −0.01575	0.9976	0.01728	0.000348
	1.0	60	a = 0.98437, k = 0.01037, c = −0.02618	0.9971	0.01799	0.000384
	1.0	70	a = 1529.88646, k = 0.00000, c = −1528.77256	0.99846	0.01468	0.00028
	1.5	40	a = 1.04247, k = 0.00829, c = −0.04144	0.9988	0.01254	0.000183
	1.5	50	a = 1.0542, k = 0.00873, c = −0.0328	0.9987	0.0156	0.00022
	1.5	60	a = 0.9915, k = 0.01012, c = −0.0217	0.9976	0.0189	0.00036
	1.5	70	a = 1.08903, k = 0.01069, c = −0.08346	0.9986	0.01304	0.000206
Two-term	0	40	a = 0.95001, k_0 = 0.00743, b = 0.06326, k_1 = 0.04600	0.9976	0.01743	0.00037
	0	50	a = 0.91772, k_0 = 0.00922, b = 0.08452, k_1 = 0.04902	0.9973	0.01786	0.00039
	0	60	a = 0.9395, k_0 = 0.01083, b = 0.03696, k_1 = 0.05269	0.9967	0.01926	0.00047
	0	70	a = 1.0634, k_0 = 0.01586, b = 0.01105, k_1 = 0.14362	0.9981	0.01592	0.00033
	0.5	40	a = 0.98849, k_0 = 0.00893, b = 0.02424, k_1 = 0.07340	0.9935	0.02873	0.00102
	0.5	50	a = 39.49319, k_0 = 0.01374, b = 38.40107, k_1 = 0.01381	0.9978	0.01815	0.00041
	0.5	60	a = 0.93954, k_0 = 0.01083, b = 0.0396, k_1 = 0.05269	0.9979	0.01520	0.00032
	0.5	70	a = 1.06343, k_0 = 0.01586, b = 0.01105, 0.14362	0.9981	0.01592	0.00033
	1.0	40	a = 48.98889, k_0 = 0.01025, b = 47.99844, k_1 = 0.01030	0.9958	0.02294	0.00064

Table 6. *Cont.*

Model	Pretreatment, % KMS	Air Temp., °C	Parameters	R^2	RMSE	χ^2
	1.0	50	a = 0.95643, k_0 = 0.00933, b = 0.05400, k_1 = 0.03736	0.9976	0.01731	0.00037
	1.0	60	a = 0.93954, k_0 = 0.01083, b = 0.03696, k_1 = 0.05269	0.9967	0.01926	0.00047
	1.0	70	a = 391.94550, k_0 = 0.01944, b = −391.42149, k_1 = 0.01958	0.99812	0.01568	0.00032
	1.5	40	a = 70.41870, k_0 = 0.01183, b = 69.41573, k_1 = 0.01188	0.9979	0.01639	0.00033
	1.5	50	a = 0.9635, k_0 = 0.00921, b = 0.0412, k_1 = 0.0526	0.9982	0.0171	0.00029
	1.5	60	a = 0.9487, k_0 = 0.01011, b = 0.0521, k_1 = 0.0613	0.9972	0.0198	0.00041
	1.5	70	a = 141.13429, k_0 = 0.01973, b = −140.14059, k_1 = 0.01980	0.9972	0.01865	0.00046
Two-term-exp	0	40	a = 0.74820, k = 0.00848	0.997	0.01944	0.00041
	0	50	a = 0.50331, k = 0.01459	0.9965	0.02059	0.00047
	0	60	a = 0.5495, k = 0.01558	0.995	0.02376	0.00063
	0	70	a = 1.6315, k = 0.01911	0.9948	0.02655	0.00079
	0.5	40	a = 1.35905, k = 0.01001	0.9936	0.02843	0.00089
	0.5	50	a = 1.75459, k = 0.01432	0.9916	0.03556	0.00141
	0.5	60	a = 0.50331, k = 0.01459	0.9952	0.02058	0.00047
	0.5	70	a = 1.63150, k = 0.01911	0.9948	0.02655	0.00079
	1.0	40	a = 1.26111, k = 0.00903	0.9957	0.02328	0.0006
	1.0	50	a = 0.85885, k = 0.00995	0.9974	0.01803	0.00036
	1.0	60	a = 0.54949, k = 0.01558	0.995	0.02376	0.00063
	1.0	70	a = 0.50331, k = 0.01459	0.99651	0.02060	0.00047
	1.5	40	a = 1.43551, k = 0.01048	0.9978	0.01662	0.00031
	1.5	50	a = 0.5126, k = 0.01387	0.9975	0.0183	0.00032
	1.5	60	a = 0.4982, k = 0.01572	0.9958	0.0236	0.00055
	1.5	70	a = 1.61526, k = 0.01623	0.9969	0.01948	0.00043
Wang–Singh	0	40	a = −0.00537, b = 0.00001	0.9736	0.05742	0.0036
	0	50	a = −0.00662, b = 0.00001	0.9567	0.07219	0.00573
	0	60	a = −0.00803, b = 1.6×10^{-5}	0.9588	0.06809	0.00518
	0	70	a = −0.00977, b = 2.3×10^{-5}	0.9747	0.05881	0.00389
	0.5	40	a = −0.00637, b = 0.00001	0.9815	0.0484	0.00259
	0.5	50	a = −0.00697, b = 0.00001	0.9823	0.05149	0.00295
	0.5	60	a = −0.00803, b = 1.5×10^{-5}	0.97345	0.06187	0.00392
	0.5	70	a = −0.00977, b = 0.00002	0.9747	0.05881	0.00389
	1.0	40	a = −0.00593, b = 0.00001	0.9785	0.05185	0.00296
	1.0	50	a = −0.00668, b = 0.00001	0.9717	0.0591	0.00386
	1.0	60	a = −0.00803, b = 0.00002	0.9588	0.06809	0.00518
	1.0	70	a = −0.00145, b = −0.00001	0.98122	0.04877	0.00285
	1.5	40	a = −0.00642, b = 0.00001	0.9848	0.04411	0.00215
	1.5	50	a = −0.00645, b = 1.12×10^{-5}	0.9784	0.0493	0.00265
	1.5	60	a = −0.00781, b = 1.64×10^{-5}	0.9635	0.0662	0.00432
	1.5	70	a = −0.00918, b = 0.00002	0.993	0.02943	0.00098
Midilli–Kucuk	0	40	a = 1.02004, k = 0.01412, n = 0.86918, b = −0.00012	0.9987	0.01258	0.00019
	0	50	a = 1.00852, k = 0.01732, n = 0.87558, b = −0.00009	0.9979	0.01573	0.0003
	0	60	a = 0.9835, k = 0.01691, n = 0.89444, b = -1.76×10^{-4}	0.9982	0.01426	0.00026
	0	70	a = 1.0723, k = 0.01724, n = 0.97788, b = -5.9×10^{-5}	0.9984	0.01487	0.00028
	0.5	40	a = 1.01673, k = 0.01408, n = 0.88582, b = −0.00022	0.9964	0.02141	0.00057
	0.5	50	a = 1.09434, k = 0.01144, n = 0.99467, b = −0.00005	0.998	0.01721	0.00037

Table 6. *Cont.*

Model	Pretreatment, % KMS	Air Temp., °C	Parameters	R^2	RMSE	χ^2
	0.5	60	a = 0.98349, k = 0.01691, *n* = 0.89444, b = −0.00018	0.99842	0.01374	0.00024
	0.5	70	a = 1.07227, k = 0.01724, *n* = 0.97788, b = −0.00006	0.9984	0.01487	0.00028
	1.0	40	a = 1.01524, k = 0.01415, *n* = 0.87433, b = −0.00020	0.9984	0.0143	0.00025
	1.0	50	a = 1.01825, k = 0.01479, *n* = 0.90123, b = −0.00012	0.9985	0.01374	0.00023
	1.0	60	a = 0.98349, k = 0.01691, *n* = 0.89444, b = −0.00018	0.9982	0.01425	0.00026
	1.0	70	a = 1.12863, k = 0.00000, *n* = 30.78936, b = 0.00058	0.99860	0.01421	0.00025
	1.5	40	a = 1.01379, k = 0.01081, *n* = 0.95146, b = −0.00014	0.999	0.0112	0.00016
	1.5	50	a = 1.0129, k = 0.01521, *n* = 0.9124, b = −0.00015	0.9991	0.0128	0.00019
	1.5	60	a = 0.9864, k = 0.01732, *n* = 0.8815, b = −0.00019	0.9983	0.0141	0.00027
	1.5	70	a = 0.99866, k = 0.00949, *n* = 1.04659, b = −0.00021	0.9985	0.01344	0.00024
Verma	0	40	a = 0.95513, k = 0.00747, g = 0.03957	0.9975	0.01781	0.00036
	0	50	a = 0.91765, k = 0.00922, g = 0.04758	0.9973	0.01787	0.00037
	0	60	a = 0.93247, k = 0.01075, g = 0.06975	0.9963	0.02041	0.0005
	0	70	a = 1.0667, k = 0.01592, g = 1.36855	0.9959	0.02382	0.00068
	0.5	40	a = 0.99417, k = 0.00897, g = 0.06585	0.9934	0.02894	0.00098
	0.5	50	a = 1.10782, k = 0.01163, g = 0.57317	0.9961	0.02424	0.00069
	0.5	60	a = 0.93247, k = 0. 01075, g = 0.03975	0.9979	0.01541	0.00033
	0.5	70	a = 1.06673, k = 0.01592, g = 1.36855	0.9958	0.02382	0.00068
	1.0	40	a = 0.98474, k = 0.00836, g = 0.06105	0.9957	0.02313	0.00062
	1.0	50	a = 0.96623, k = 0.00941, g = 0.03308	0.9975	0.0176	0.00036
	1.0	60	a = 0.93247, k = 0.01075, g = 0.06974	0.9963	0.02041	0.0005
	1.0	70	a = 260.62621, k = 0.01717, g = 0.01730	0.99805	0.01594	0.00034
	1.5	40	a = 1.01858, k = 0.00933, g = 0.24549	0.9977	0.01725	0.00035
	1.5	50	a = 0.9586, k = 0.00918, g = 0.0485	0.9978	0.0176	0.0003
	1.5	60	a = 0.9412, k = 0.01005, g = 0.0634	0.9967	0.0212	0.00048
	1.5	70	a = 138.02493, k = 0.01951, g = 0.01958	0.9972	0.01878	0.00043
Diffusion	0	40	a = 0.04487, k = 0.03957, b = 0.18873	0.9975	0.01781	0.00036
	0	50	a = 0.08234, k = 0.04758, b = 0.19377	0.9973	0.01787	0.00037
	0	60	a = 0.06753, k = 0.06975, b = 0.15409	0.9963	0.02041	0.0005
	0	70	a = 54.8398, k = 0.00964, b = 0.99245	0.9942	0.0282	0.00095
	0.5	40	a = −55.13675, k = 0.01128, b = 0.99590	0.9937	0.0283	0.00094
	0.5	50	a = 61.54936, k = 0.00603, b = 0.99163	0.989	0.04066	0.00195
	0.5	60	a = 0.06753, k = 0.06975, b = 0.1509	0.9960	0.02159	0.00060
	0.5	70	a = 54.83980, k = 0.00963, b = 0.99245	0.9942	0.0282	0.00095
	1.0	40	a = −38.17571, k = 0.00988, b = 0.99617	0.9957	0.02323	0.00063
	1.0	50	a = 0.03377, k = 0.03308, b = 0.28433	0.9975	0.0176	0.00036
	1.0	60	a = 0.06753, k = 0.06975, b = 0.15409	0.9963	0.02041	0.0005
	1.0	70	a = 226.97093, k = 0.01716, b = 1.00851	0.99600	0.02161	0.00060
	1.5	40	a = 0.79883, k = 0.00908, b = 1.00002	0.9973	0.01854	0.0004
	1.5	50	a = 0.0618, k = 0.0412, b = 0.2156	0.9972	0.0191	0.00034
	1.5	60	a = 0.0725, k = 0.0527, b = 0.1834	0.9965	0.0216	0.0005
	1.5	70	a = 55.82163, k = 0.00709, b = 0.98944	0.9988	0.01217	0.00018

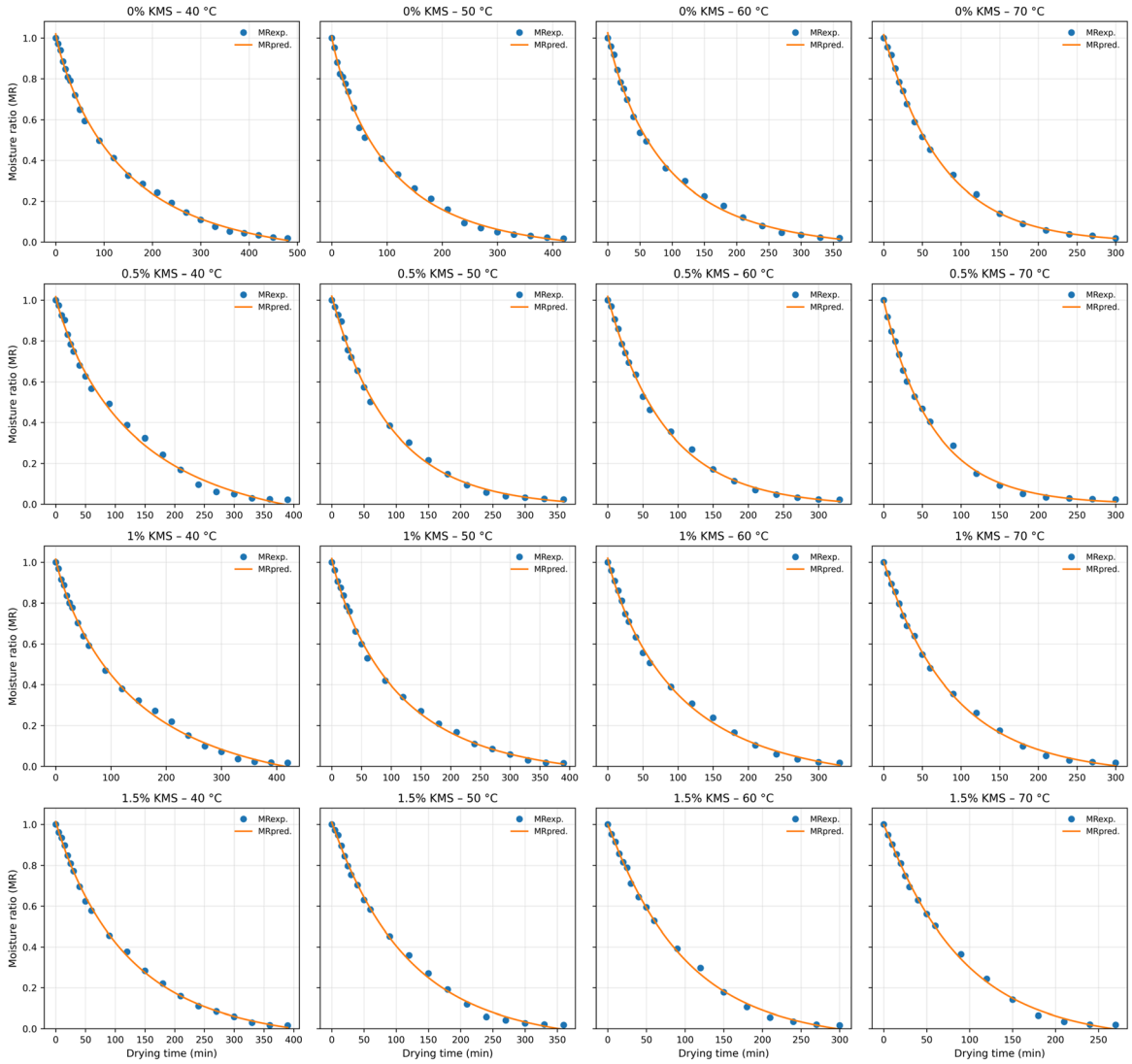


Figure 7. Experimental (MRexp.) and predicted (MRpred.) moisture ratio as a function of drying time for green banana slices subjected to different KMS pretreatments and drying temperatures using the Midilli–Kucuk model.

4. Conclusions

The combined effects of drying temperature and KMS pretreatment demonstrate that moisture removal from green banana slices was predominantly controlled by falling-rate behaviour. Apparent effective moisture diffusivity increased from 2.04×10^{-10} to 4.35×10^{-10} m^2/s across the investigated conditions, while apparent activation energy decreased from 16.19 kJ/mol for the untreated control to 13.46 kJ/mol at 1.5% KMS. The thermodynamic analysis gave ΔH values of 10.61–13.59 kJ/mol, negative ΔS values of -209.15 to -219.72 J/mol·K, and positive ΔG values of 76.35–87.73 kJ/mol, indicating a non-spontaneous process requiring external thermal energy input. The time required to reach an interpolated 10% d.b. moisture content ranged from 227.0 to 437.6 min and provides a more appropriate basis for treatment comparison than the differing endpoint drying times. Among the ten models evaluated, Midilli–Kucuk gave the best overall goodness of fit within the investigated range, but its superiority should be regarded as condition-specific. The main limitations are the absence of direct equilibrium-moisture measurement, the use of an apparent infinite-slab diffusivity approximation, and the lack of direct measurements of electrical energy consumption and operating cost. Future work should therefore combine KMS pretreatment with energy/exergy analysis, product-quality

assessment, independently replicated drying runs with replicate-level uncertainty, and validation at a common target moisture content under pilot-scale conditions.

Author Contributions: K.P.D.: Conceptualisation, Data Curation, Formal Analysis, Investigation, Methodology, Visualisation, Validation, Writing—Original Draft. S.K.J.: Conceptualisation, Formal Analysis, Resources, Supervision, Validation Writing—Review and Editing. P.B.P.: Conceptualisation, Formal Analysis, Visualisation, Validation Writing—Review and Editing. S.D.P.: Formal Analysis, Visualisation, Writing—Review and Editing. All authors have read and agreed to the published version of the manuscript.

Funding: This research received no external funding.

Institutional Review Board Statement: Not applicable.

Informed Consent Statement: Not applicable.

Data Availability Statement: The original contributions presented in the study are included in the article; further inquiries can be directed to the corresponding author.

Acknowledgments: The corresponding author gratefully acknowledges the Deanship of Research, Sultan Qaboos University, Oman, for supporting this research under the Internal Research Grant (Grant No. IG/DVC/ITTC/24/01).

Conflicts of Interest: The authors declare no conflicts of interest.

References

1. Pareek, S. Nutritional and Biochemical Composition of Banana (*Musa* spp.) Cultivars. In *Nutritional Composition of Fruit Cultivars*; Elsevier: Amsterdam, The Netherlands, 2016; pp. 49–81.
2. Rodríguez-Miranda, J.; Martínez-Sánchez, C.E.; Hernández-Santos, B.; Juárez-Barrientos, J.M.; Ventura-Báez, E.G.; Herman-Lara, E. Effect of Enzymatic Pretreatment on the Physical Quality of Plantain (*Musa* ssp., Group AAB) Employing Airflow Reversal Drying. *J. Food Sci. Technol.* **2018**, *55*, 157–163. [CrossRef] [PubMed]
3. Dhake, K.; Jain, S.K.; Jagtap, S.; Pathare, P.B. Effect of Pretreatment and Temperature on Drying Characteristics and Quality of Green Banana Peel. *AgriEngineering* **2023**, *5*, 2064–2078. [CrossRef]
4. Al-Dairi, M.; Pathare, P.B.; Al-Yahyai, R.; Jayasuriya, H.; Al-Attabi, Z. Postharvest Quality, Technologies, and Strategies to Reduce Losses along the Supply Chain of Banana: A Review. *Trends Food Sci. Technol.* **2023**, *134*, 177–191. [CrossRef]
5. Padhi, S.; Murakonda, S.; Dwivedi, M. Investigation of Drying Characteristics and Nutritional Retention of Unripe Green Banana Flour by Refractance Window Drying Technology Using Statistical Approach. *J. Food Meas. Charact.* **2022**, *16*, 2375–2385. [CrossRef]
6. Kumar, R.; Pandey, O.P.; Dhiman, S.K.; Kumar, P. Influence of Blanching and Drying Air Temperature on Drying Kinetics of Banana Slices. *J. Biosyst. Eng.* **2021**, *46*, 375–385. [CrossRef]
7. Kaur, K.; Singh, G.; Singh, N. Functional, Pasting, Nutritional and Gluten Free Muffin Making Properties of Plantain Flour. *Asian J. Dairy Food Res.* **2018**, *37*, 298–303. [CrossRef]
8. Olalekan, A.S.A. *Banana Drying Kinetics*; Anyasi, T.A., Ed.; IntechOpen: Rijeka, Croatia, 2020; pp. 1–20, ISBN 978-1-83968-528-6.
9. Wijerathne, A.D.H.T.; Joardder, M.U.H.; Welsh, Z.G.; Nayak, R.; Sablani, S.S.; Karim, A. Recent Advances in Food Drying Modeling: Empirical to Multiscale Physics-Informed Neural Networks. *Compr. Rev. Food Sci. Food Saf.* **2025**, *24*, e70194. [CrossRef] [PubMed]
10. Gómez-de la Cruz, F.J.; Palomar-Torres, A.; Torres-Jiménez, E.; Cruz-Peragón, F. Drying Kinetics of Crushed Mango Stone: Analysis of Effective Moisture Diffusivity and Drying Rate for Any Drying Condition. *Therm. Sci. Eng. Prog.* **2026**, *71*, 104571. [CrossRef]
11. Rani, P.; Tripathy, P.P. Effect of Ultrasound and Chemical Pretreatment on Drying Characteristics and Quality Attributes of Hot Air Dried Pineapple Slices. *J. Food Sci. Technol.* **2019**, *56*, 4911–4924. [CrossRef] [PubMed]
12. Kamal, M.M.; Ove, T.A.; Saifullah, S.B.; Haque, M.R. Effects of Citric Acid and Potassium Metabisulphite Pre-Treatment on the Physical and Biochemical Properties of Dehydrated Amritsagar Banana Powder. *Trends Sci.* **2022**, *19*, 2893. [CrossRef]
13. Martínez, S.; Roman-Chipantiza, A.; Boubertakh, A.; Carballo, J. Banana Drying: A Review on Methods and Advances. *Food Rev. Int.* **2024**, *40*, 2188–2226. [CrossRef]
14. AOAC International. *Official Methods of Analysis of the Association of Official Analytical Chemists International*, 20th ed.; AOAC International: Rockville, MD, USA, 2016.

15. Sarpong, F.; Yu, X.; Zhou, C.; Hongpeng, Y.; Uzoejinwa, B.B.; Bai, J.; Wu, B.; Ma, H. Influence of Anti-Browning Agent Pretreatment on Drying Kinetics, Enzymes Inactivation and Other Qualities of Dried Banana (*Musa* ssp.) under Relative Humidity-Convective Air Dryer. *J. Food Meas. Charact.* **2018**, *12*, 1229–1241. [CrossRef]
16. Dhake, K.P.; Jain, S.K.; Jagtap, S.; Pathare, P.B. Optimization of Drying Parameters for Pretreated Green Banana Slices Using Response Surface Methodology. *J. Food Qual.* **2025**, *2025*, 3959937. [CrossRef]
17. Omolola, A.O.; Jideani, A.I.O.; Kapila, P.F. Modeling of Thin Layer Drying Characteristics of Banana *cv. Luvhele*. *Bulg. J. Agric. Sci.* **2015**, *21*, 342–348.
18. Narasingam, K.S.P.; Murugan, N.; Celliyamman Velusamy, V.; Karuppuchamy, V.; Karunakaran, K.; Saravanan, J. Open Sun and Cabinet Drying of Whole Tamarind Fruit and Its Modeling Approach. *J. Food Process Eng.* **2026**, *49*, e70413. [CrossRef]
19. Mghazli, S.; Ouhammou, M.; Hidar, N.; Lahnine, L.; Idlimam, A.; Mahrouz, M. Drying Characteristics and Kinetics Solar Drying of Moroccan Rosemary Leaves. *Renew. Energy* **2017**, *108*, 303–310. [CrossRef]
20. Gadhave, R.K.; Kaur, R.; Das, R.; Prasad, K. Dehydration Kinetics of Green Banana Slices, Characterization of Optimized Product Based on Physicochemical, Nutritional, Optical, and Sensory Attributes. *J. Appl. Biol. Biotechnol.* **2023**, *11*, 82–93. [CrossRef]
21. Togrul Turk, I.; Pehlivan, D. Mathematical Modelling of Solar Drying of Apricots in Thin Layers. *J. Food Eng.* **2002**, *55*, 209–216. [CrossRef]
22. Olawoye, B.T.; Kadiri, O.; Babalola, T.R. Modelling of Thin-Layer Drying Characteristic of Unripe Cardaba Banana (*Musa* ABB) Slices. *Cogent Food Agric.* **2017**, *3*, 1290013. [CrossRef]
23. Kumar, P.S.; Nambi, E.; Shiva, K.N.; Vaganan, M.M.; Ravi, I.; Jeyabaskaran, K.J.; Uma, S. Thin Layer Drying Kinetics of Banana Var. Monthan (ABB): Influence of Convective Drying on Nutritional Quality, Microstructure, Thermal Properties, Color, and Sensory Characteristics. *J. Food Process Eng.* **2019**, *42*, e13020. [CrossRef]
24. Macedo, L.L.; Vimercati, W.C.; da Silva Araújo, C.; Saraiva, S.H.; Teixeira, L.J.Q. Effect of Drying Air Temperature on Drying Kinetics and Physicochemical Characteristics of Dried Banana. *J. Food Process Eng.* **2020**, *43*, e13451. [CrossRef]
25. Al-Amin, M.; Hossain, M.; Iqbal, A. Effect of Pre-Treatments and Drying Methods on Dehydration and Rehydration Characteristics of Carrot. *Univers. J. Food Nutr. Sci.* **2018**, *3*, 23–28. [CrossRef]
26. Gao, J.; Chen, L.; Zeng, X.; Sun, X.; Bai, Y.; Wang, X.; Xu, X.; Han, M. Novel Drying Pretreatment Technologies and Their Applications in the Food Industry. *Food Mater. Res.* **2023**, *3*, 14. [CrossRef]
27. Kamble, M.; Singh, A.; Kumar, N.; Dhenge, R.; Rinaldi, M.; Chinchkar, A. Semi-Empirical Mathematical Modeling, Energy and Exergy Analysis, and Textural Characteristics of Convectively Dried Plantain Banana Slices. *Foods* **2022**, *11*, 2825. [CrossRef] [PubMed]
28. Zeng, Z.; Han, C.; Wang, Q.; Yuan, H.; Zhang, X.; Li, B. Analysis of Drying Characteristic, Effective Moisture Diffusivity and Energy, Exergy and Environment Performance Indicators during Thin Layer Drying of Tea in a Convective-Hot Air Dryer. *Front. Sustain. Food Syst.* **2024**, *8*, 1371696. [CrossRef]
29. Taiwo, K.A.; Babalola, R.T. Studies on the Drying Kinetics and Rehydration Capacities of Cardaba Banana Compared to Plantain Slices. *Open Agric.* **2018**, *3*, 57–71. [CrossRef]
30. Fawohunre, A.; Adewumi, B.; Ou, D.; Sobukola, O. Fittingmodel for the Thin Layer Drying of Plantain (*Musa acuminata*). *Am. J. Eng. Res.* **2019**, *8*, 160–166.
31. Khawas, P.; Das, A.J.; Dash, K.K.; Deka, S.C. Thin-Layer Drying Characteristics of Kachkal Banana Peel (*Musa* ABB) of Assam, India. *Int. Food Res. J.* **2014**, *21*, 1011–1018.
32. Pinheiro, M.N.C.; Castro, L.M.M.N. Effective Moisture Diffusivity Prediction in Two Portuguese Fruit Cultivars (Bravo de Esmolfe Apple and Madeira Banana) Using Drying Kinetics Data. *Heliyon* **2023**, *9*, e17741. [CrossRef] [PubMed]
33. Tuncer, A.D.; Güler, H.Ö.; Usta, H. Modeling of Drying Characteristics of Pomelo (*Citrus maxima*) Peel. *El-Cezeri J. Sci. Eng.* **2020**, *7*, 198–210. [CrossRef]
34. Doymaz, I. Evaluation of Mathematical Models for Prediction of Thin-Layer Drying of Banana Slices. *Int. J. Food Prop.* **2010**, *13*, 486–497. [CrossRef]

Disclaimer/Publisher's Note: The statements, opinions and data contained in all publications are solely those of the individual author(s) and contributor(s) and not of MDPI and/or the editor(s). MDPI and/or the editor(s) disclaim responsibility for any injury to people or property resulting from any ideas, methods, instructions or products referred to in the content.